Object detection in images with low light condition

Kvyetnyy, Roman, Maslii, Roman, Harmash, Volodymyr, Bogach, Ilona, Kotyra, Andrzej, et al.

Roman Kvyetnyy, Roman Maslii, Volodymyr Harmash, Ilona Bogach, Andrzej Kotyra, Żaklin Grądz, Aizhan Zhanpeisova, Nursanat Askarova, "Object detection in images with low light condition," Proc. SPIE 10445, Photonics Applications in Astronomy, Communications, Industry, and High Energy Physics Experiments 2017, 104450W (7 August 2017); doi: 10.1117/12.2281001

SPIE.

Event: Photonics Applications in Astronomy, Communications, Industry, and High-Energy Physics Experiments 2017, 2017, Wilga, Poland

Object detection in images with low light condition

Roman Kvyetnyy*[a], Roman Maslii[a], Volodymyr Harmash[a], Ilona Bogach[a], Andrzej Kotyra[b], Żaklin Grądz[b], Aizhan Zhanpeisova[c], Nursanat Askarova[d]
[a]Vinnytsia National Technical University, 95 Khmelnitsky Shose Str., 21000 Vinnytsia, Ukraine; [b]Lublin University of Technology, Nadbystrzycka 38a, 20-618 Lublin, Poland; [c]M.Kh. Dulaty Taraz State University, 7 Suleymenov str., 080012 Taraz, Kazakhstan; [d]Kazakh National Research Technical University after K. I. Satpaev, 22 Satbaev Str., 050013 Almaty, Kazakhstan

ABSTRACT

Images acquired by computer vision systems under low light conditions are characterized by the existence of noises. As a rule, it results in decreasing object detection rate. To increase the object detection rate, the proper image preprocessing algorithm is needed. The paper presents the image denoising method based on bilateral filtering and wavelet thresholding. The boosting method for object detection that uses the modified Haar-like features which include Haar-like features and symmetrical local binary patterns are proposed. The proposed algorithm allows increasing object detection rate in comparison with Viola-Jones method for a case of face detection task. The algorithm was tested on the two image sets, Yale B and the proprietary – VNTU-458.

Keywords: object detection, image denoising, wavelet thresholding, bilateral filtering

1. INTRODUCTION

Object detection is one of the main purposes of image analysis in computer vision systems. Under the low light condition, the images acquired are characterized by the existence of noises. It causes not only the degradation of image visual perception but also the decreasing of object detection rate.

Image denoising is usually connected with filtering operation. There exist a number of known image denoising methods as: Gaussian smoothing model[1], Yaroslavsky neighborhood filter[2], SUSAN (Smallest Univalue Segment Assimilating Nucleus) filter[3], bilateral filter[4]; PDE based methods: anisotropic filtering model[5], Rudin-Osher-Fatemi total variation model[6]; filters in frequency domain: hard and soft thresholding[7,8], Zhou-Wang wavelet total variation[9], curvelet denoising[10] and non-local means algorithm[11].

The analysis of image denoising methods allows drawing a conclusion that most of them are focused on grayscale images with additive artificial noise. Only a few are assigned to images received by a digital camera with real noise. Noise in a digital image has a low frequency (coarse-grain) and high frequency (fine-grain) components. The high-frequency components are typically easier to remove but it is difficult to distinguish between the real signal and the low-frequency noise. Perspective methods for enhancing image quality are methods that based on wavelet transform and bilateral filter method[12]. Wavelet transform based method perfectly finds both low-frequency and high-frequency components of a signal in different time scales allowing better distinguishing of noise and image information at every decomposition level. Bilateral filter method is applying weighted spatial averaging without smoothing the boundaries[4]. Lately, the best results of object detection are showing methods which consider the object detection task as a binary classification task, namely the classification of two classes: "the object" and "not the object". Such a classifier performs exhaustive search rectangular image fragments of all sizes and conducting of verification of each fragment for object existence[13]. Among the mentioned methods are the naive Bayes classifier[14], neural networks[15], boosting methods[16], etc.

Great attention is paid to boosting methods[16-18] because they can process the image on a real-time basis and are effective according to the criteria for the first and the second type errors. Haar-like features or their modification are used in numerous boosting-methods. The main advantage of these methods is the simplicity of evaluation. On the other side, their disadvantage consists in the sensitiveness to the light conditions[19].

*rkvetny@sprava.net

Photonics Applications in Astronomy, Communications, Industry, and High Energy Physics Experiments 2017, edited by Ryszard S. Romaniuk, Maciej Linczuk, Proc. of SPIE Vol. 10445, 104450W
 · doi: 10.1117/12.2281001

For creating boosting method with high object detection rate the set of features being robust to light conditions should be applied. Among such features, local binary patterns[20] (LBP) is worth mentioning. For speeding up the image processing, it is reasonable to apply the set of features which combines LBP and Haar-like features[21].

The aim of the research presented is the development of the object detection method in images with low light conditions that would allow increasing the object detection rate. The method will be tested on face detection task. The proposed method consists of two stages: the first is the previous processing of grayscale images with denoising method that is based on bilateral filter and wavelet thresholding (BWIF). The second stage is boosting method of object detection in grayscale images (BODM).

2. IMAGE DENOISING METHOD

Let there be given a noisy grayscale image $u'(x, y)$ of size $M \times N$. The image is decomposed into its frequency subbands by the wavelet decomposition. After wavelet decomposition, the image is decomposed into the approximate subband and the detail subband. The detail subband is consisting of horizontal, vertical and diagonal parts. Since coarse-grained noise is difficult to determine and remove at the high-frequency level, the image is decomposed into subbands where the noise is transformed into the fine-grained and can be removed at the low-frequency level.

Coefficients of approximation of function $u`(x, y)$ in the starting scale are determined as follows[22]:

$$W_{\varphi}(j_0, m, n) = \frac{1}{\sqrt{MN}} \sum_{x=0}^{M-1} \sum_{y=0}^{N-1} u'(x, y) \varphi_{j_0,m,n}(x, y) \tag{1}$$

where j_0 is arbitrary starting scale, $\varphi_{j_0,m,n}(x, y)$ – scaling function. Coefficients which represent horizontal (H), vertical (V) and diagonal (D) parts for scales are determined as follows:

$$W^s{}_{\psi}(j, m, n) = \frac{1}{\sqrt{MN}} \sum_{x=0}^{M-1} \sum_{y=0}^{N-1} u'(x, y) \psi^s{}_{j,m,n}(x, y) \tag{2}$$

where $s = \{H, V, D\}$, $\psi^s{}_{j,m,n}(x, y)$ are wavelet functions. Bilateral filtering is applied to the approximate subband $W_{\varphi}(j_0, m, n)$. For image $u'(x, y)$ at pixel x, the bilateral filter is determined as follows:

$$BF = \frac{1}{C} \sum\nolimits_{y \in N(x)} e^{\frac{-\|y-x\|^2}{2\sigma^2 d}} e^{\frac{-|u'(y)-u'(x)|^2}{2\sigma^2 r}} u'(y) \tag{3}$$

where σ_d and σ_r are parameter determination of weight in spatial domain and domain of intensity; $N(x)$ is spatial neighbor of pixel; C is the normalization coefficient:

$$C = \sum\nolimits_{y \in N(x)} e^{\frac{-\|y-x\|^2}{2\sigma^2 d}} e^{\frac{-|u'(y)-u'(x)|^2}{2\sigma^2 r}} \tag{4}$$

The result of bilateral filtering is the calculation of the intensity of every pixel as a weighted average of the neighboring pixel intensities. The weight related to each neighboring pixel changes according to the concerns of distances on image area (spatial weight) and on the axis of intensity (ranking weight) which allows saving precise limits of image elements.

Applying Normal Shrink thresholding technique to the detail subband $W^i{}_{\psi}(j, m, n)$. The threshold value is determined as follows:

$$T_N = \frac{\mu \hat{\sigma}^2}{\hat{\sigma}_y} \tag{5}$$

where μ is scale parameter:

$$\mu = \sqrt{\log(\frac{L_z}{J})} \tag{6}$$

where L_z is the length of the subband in z^{th} scale; J is a general number of decomposition levels; $\hat{\sigma}^2$ - the noise variance which is calculated from the subband HH1:

$$\hat{\sigma}^2 = \left[\frac{median(|Y_{ij}|)}{0{,}6745} \right]^2 \tag{7}$$

Where Y_{ij} is wavelet coefficient of the subband HH1 and $\hat{\sigma}_y$ is the standard deviation of the subband.

Let's apply threshold processing for horizontal, vertical and diagonal parts where the components of noise can be effectively defined and removed. The image is reconstructed back using inverse wavelet transform. The reconstructed image $\tilde{u}(x, y)$ is obtained via inverse discrete wavelet transform using expression (1) and (2):

$$\tilde{u}(x,y) = \frac{1}{\sqrt{MN}} \sum_m \sum_n W_\varphi(j_0,m,n)\varphi_{j_0,m,n}(x,y) + \frac{1}{\sqrt{MN}} \sum_{i=H,V,D} \sum_{j=j_0}^{\infty} \sum_m \sum_n W^s{}_\psi(j,m,n)\psi^s{}_{j,m,n}(x,y) \tag{8}$$

After the image has been reconstructed, the bilateral filter can be applied toward it again. In the result of processing, we get denoising image $u''(x, y)$. Scheme of image denoising process for two levels of decomposition is shown in figure 1.

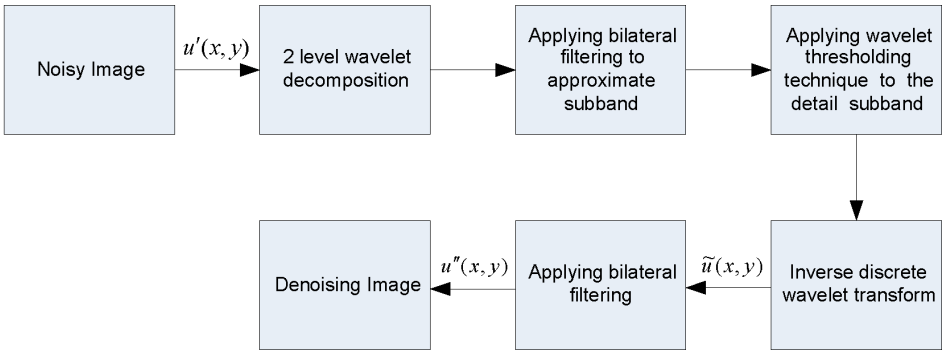

Figure 1. Scheme of image denoising process.

3. BOOSTING OBJECT DETECTION METHOD

Haar-like features are determined in grayscale image. The feature value is defined as the difference of the sum of pixels' intensity of areas inside the rectangle, which can be at any position and scale within the original image (fig. 2).

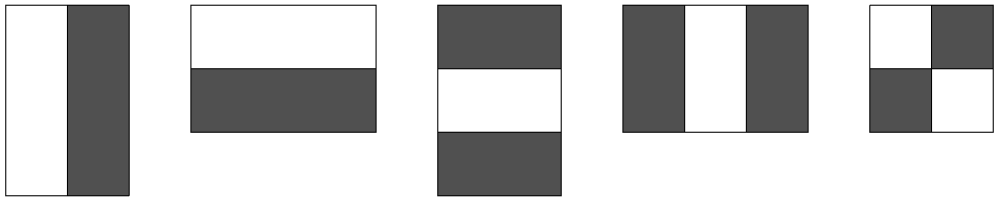

Figure 2. Haar-like features.

Local binary pattern (LBP) is represented by description of neighborhood of pixel image in the binary form[20]. The meaning of symmetrical local binary pattern (SLBP) in applying to neighborhood of grayscale pixel image at (x,y) coordinates can be described as[23]:

$$CS-LBP(x,y)=\sum_{p=0}^{(Np/2)-1} s(k_p-k_{p+Np/2})2^p\,, \tag{9}$$

where N_p is the number of pixel neighborhood; k is the meaning of pixel neighborhood intensities;

$$s(k_p-k_{p+Np/2})=\begin{cases}1, & if \quad k_p-k_{p+Np/2}>\lambda\\ 0, & else\end{cases}, \tag{10}$$

where λ is the threshold.

According to the formula (9) SLBP operator, which is applied to pixel neighborhood of grayscale image with coordinates (x, y), using eight pixels in the neighborhood ($k0 – k7$) composes of four-unit code (fig. 3).

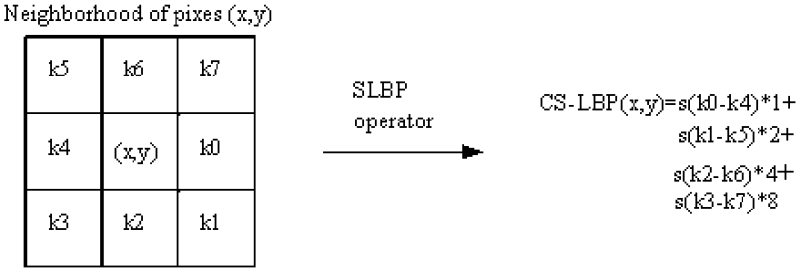

Figure 3. Calculation of the value of SLBP feature.

The new set of features that uses SLBP features and Haar-like features are called the modified Haar-like features (MHF). To calculate MHF the grayscale image is transformed into SLBP array and then transformed into a set of integral SLBP array (ILBP) according to the following expression:

$$i_d(x,y)=i_d(x,y-1)+\delta_d(x,y) \tag{10}$$

$$I_d(x,y)=I_d(x-1,y)+i_d(x,y) \tag{11}$$

where I is ILBP array; i is auxiliary array, d = 1,…,16; $\delta_d(x, y)$ = 1, if array cell out of the set I^P_{LBP} with coordinates (x, y) equals d, and $\delta_d(x, y)$ = 0 in another case.

The MHF feature is determined by such set of parameters: type of Haar-like feature (fig.2.1), SLBP value, size and location in the image, which correspond to the size of minimal sliding window (for example, 24×24 pixel). Calculating SLBP values according to the expression (9) of all the pixels of grayscale image except interfacial it is possible do determine SLBP array (fig. 4)

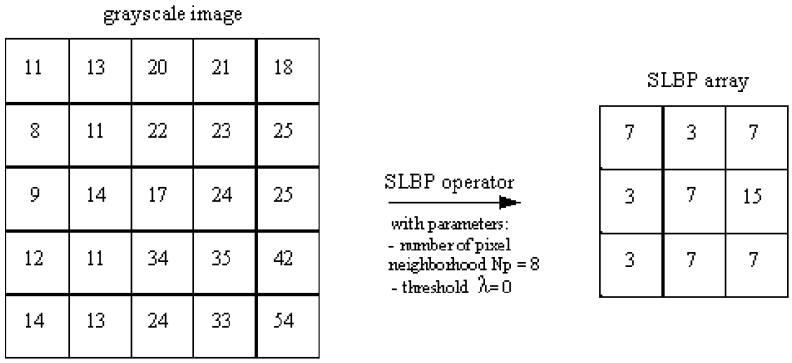

Figure 4. Getting SLBP array from grayscale image.

Sample of getting a set of ILBP arrays from SLBP array is shown on fig.5. According to MHF parameters, using the appropriate ILBP array I, number of SLBP features is calculated in light and dark rectangles of MHF. MHF value is calculated as follows:

$$f(I) = S_W - S_B \tag{12}$$

where S_W – number of SLBP features in light rectangles of MHF, S_B – number of SLBP features in dark rectangles of MHF , I – ILBP array. The values S_W and S_B is calculated as follows:

$$S = I(a_2, b_2) - I(a_3, b_3) - I(a_1, b_1) + I(a_4, b_4) \tag{13}$$

where (a_1,b_1), (a_2,b_2), (a_3,b_3), (a_4,b_4) – are the coordinates of four pixels connected with the appropriate rectangle in MHF (neighboring on top with right upper pixel of rectangle, right lower pixel of triangle, neighboring on the left with left lower pixel of rectangle, neighboring on the diagonal on top with left upper pixel of rectangle).

To enhance processing speed cascade of strong classifiers (CSC) are applied. MHF is used as simple classifiers. Elaboration of object detection technique consists of several stages[22]:
1) training of CSC on a set of examples;
2) image classification with CSC;
3) verification of candidate-regions.

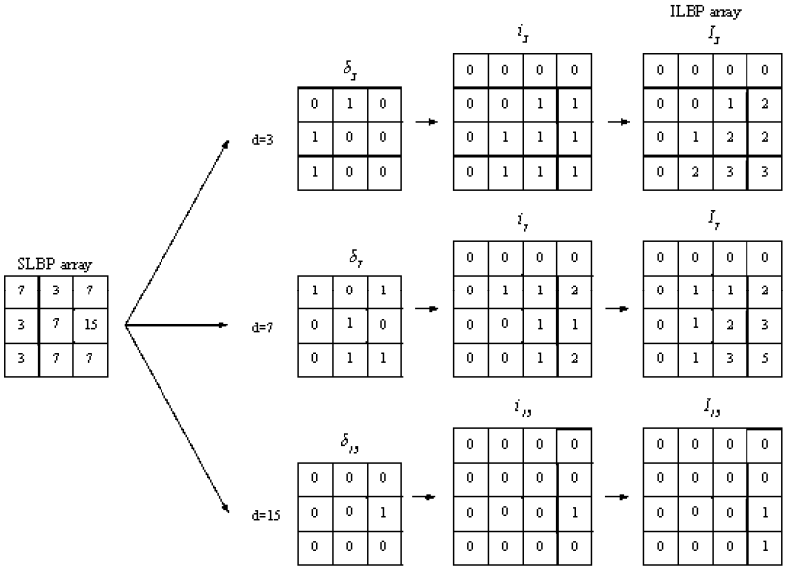

Figure 5. Getting the set of ILBP array from SLBP array.

3.1 The stage of CSC training

Implementation of the first stage requires sets of positive and negative examples. Therefore, basis of object images B_{object}, as well as the basis of images on which there are no objects $B_{non\text{-}object}$ are created.
The images from B_{object} is normalized and out of it training P and verification sets V_p of positive examples are created. Image regions are extracted from $B_{non\text{-}object}$ and training P and verification sets V_p of negative examples are formed. Images in P V_p, N, V_n sets are scaled to minimal sliding window.

For CSC is established the certainly value of false positive rate FP_C and certainly value of true positive rate TP_C, to which CSC has to achieve during the training. Strong classifiers will be added to CSC for as long as the determined FP_C and TP_C are achieved.

From the set of positive training examples at the application of SLBP operator the set of SLBP arrays of positive examples I^P_{LBP} is obtained. In a similar manner, from the set of negative training examples we get the set of SLBP arrays

of negative examples I^N_{LBP}. Applying the expressions (10) and (11) from the set I^P_{LBP} we get the set of ILBP arrays of positive examples I^P, and from I^N_{LBP} set we get the set of ILBP arrays of negative examples I^N.

Using I^P and I^N sets, the value of each MHF f_j is calculated. Its optimal threshold θ_j, and the direction of sign p_j are determined. For each strong classifier, exact value of false positive rate *FP* is established, and exact value of true positive rate *TP*, to which the strong classifier has to achieve during the training.

The training of each strong classifier will be accomplished until achievement of the determined *FP* and *TP*. The training sample is formed by I^P_{LBP} set of positive examples and I^N_{LBP} set of negative examples in a following form: $(x_1, y_1),\ldots,(x_n, y_n)$, where x is SLBP array, y – objective value that equals 0 – for the negative examples, 1 – for the positive examples. Initialization of weight $w_{1,I} = 1/2m$, $1/2l$, for $y_i = 0$, 1 accordingly, where m – number of positive examples, l – number of negative examples, and currently value of false positive rate *fpRate* (initially *fpRate*=1). A cycle is activated with a condition while *fpRate* > *FP*, where t denotes the current iteration, I – index of example, j – MHF index.

The weight examples of training sample are normalized:

$$w_{t,i} \leftarrow \frac{w_{t,i}}{\sum_{k=1}^{n} w_{t,k}} \tag{14}$$

The simple classifier h_j for each MHF using I^P and I^N is formed according to the following expression:

$$h_j(x) = \begin{cases} 1, & if \quad p_j f_j(x) < p_j \theta_j \\ 0, & else \end{cases} \tag{15}$$

where f_j – MHF, x – SLBP array, θ_j – threshold, p_j – direction of MHF sign. The error of all simple classifier in training sample is calculated as:

$$\varepsilon_j = \sum_i w_i \left| h_j(x_i) - y_i \right| \tag{16}$$

To the strong classifier, the simple classifier h_t is added with the smallest error ε_t. Weight examples are renewed according to the expression:

$$w_{t+1,i} = w_{t,i} \beta_t^{1-e_i} \tag{17}$$

where $e_i = 0$ if the example x_i is defined correctly, $e_i = 1$ otherwise, $\beta_t = \frac{\varepsilon_t}{1-\varepsilon_t}$. The strong classifier is defined as:

$$h(x) = \begin{cases} 1, & if \quad \sum_{t=1}^{T} \alpha_t h_t(x) \geq \xi \\ 0, & else \end{cases} \tag{18}$$

where $\alpha_t = \log \frac{1}{\beta_t}$, $\xi = \frac{1}{2} \sum_{t=1}^{T} \alpha_t$.

Using verification set of positive examples V_p, threshold ξ of strong classifier is adjusted for reaching the defined value of true positive rate *TP*. It is calculated the certainly value of false positive rate *fpRate* of strong classifier on verification set of negative examples V_n. Transition into next iteration of the cycle is accomplished in case of implementation the condition *fpRate* > *FP*, otherwise, strong classifier is added to CSC.

It is accomplished the transition to the next strong classifier. To form the set of negative examples N of the next strong classifier is extracted from $B_{non\text{-}face}$ image region which are scaled to minimal sliding window and negative examples are

formed out of them. Transformation of image region into ILBP array is accomplished and placed to the CSC input. The examples, that CSC has taken as positive are added to set *N*.

3.2 Image classification with CSC

Classification with CSC for object detection is accomplished in the following way. Input image is transformed into SLBP array and according to the expressions (10) and (11) 16 ILBP arrays are produced. Sliding window, the size of which equals to minimal and then increases by coefficient M_s, at scale change, moves along image rows with step K_r pixels. The image region is extracted and corresponding to it parts of ILBP arrays are placed at CSC input. In case of strong classifier, using the obtained parts of ILBP arrays according to expression (15) is calculated MHF value in simple classifiers. According to the expression (18) a decision is made on the transition to the next strong classifier in a cascade in the case $h(x) = 0$, or to the rejection of current image region in the case $h(x) = 1$ and the transition to processing of the next image region, extracted by sliding window. In the case when all strong classifiers of the cascade will make decision on $h(x) = 1$ image region is considered as an object.

3.3 The stage of verification of candidate-regions

CSC is marked out on the image several defined regions – candidate-regions, after passing the sliding window through the whole image in all scales. For verification of candidate-regions the rule of clustering is applied, in which all variety of candidate-regions are broken up for varieties, which are not intersected. At clustering two candidate-regions are related to one cluster, if they are intersected by more than percent ϕ. Cluster is a candidate for creating united region if the variety of candidate-regions is more than threshold *Thr*. United region is formed by finding arithmetic average of coordinates of candidate-regions, that are included into a cluster. Each of united regions is determined as object region[24].

4. EXPERIMENT RESULTS

During experiments test set of 640 grayscale images was used. The set was retrieved from "Yale B" database, where images are characterized by wide range of changes of light conditions (fig. 6 a). Another test set that was used during the experiments was set of 458 grayscale images recorded by the authors in Vinnytsya National Technical University campus under low light conditions (VNTU-458) (fig. 6 b).

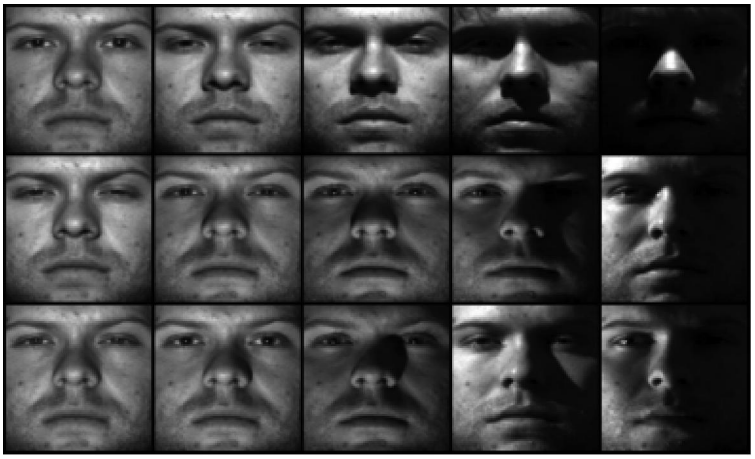

a)

b)

Figure 6. Samples of images: a) facial region from test set from "Yale B"; b) test set from VNTU-458.

For object detection method evaluation ROC-curves were used. Object detection rate (true positive rate) is determined as a quotient of number parts of image which the classifier defined as the object to general number parts of image which are the objects. Number of false detection (false positive) is defined as a number of parts of image which the classifier defined as the object in case if they are not the objects. To form ROC-curves the approach[16] was applied, according to which the adjusting of threshold ψ in SC (18) is performed for receiving number of false positives (in the range 10 to 120) and object detection rate (correct detection rate).

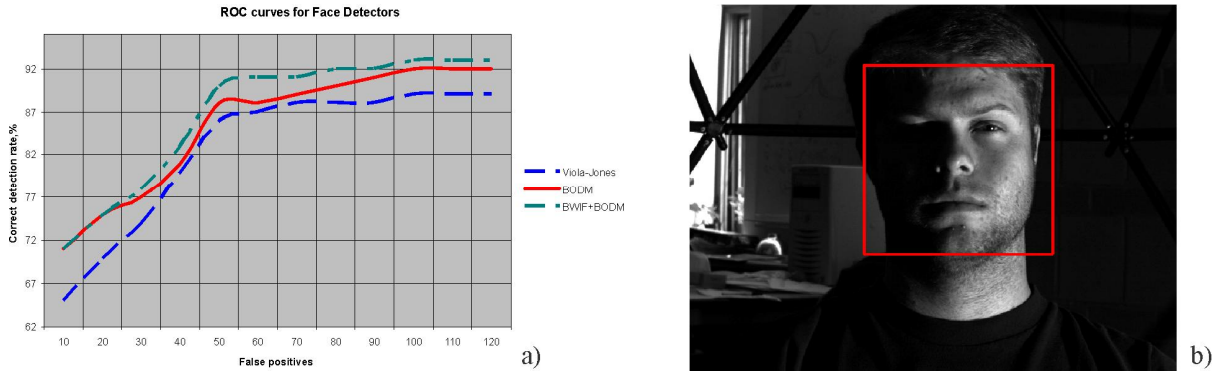

Figure 7. The research results of object detection on test set from the base "Yale B": a) ROC-curves of detection methods; b) the example of face detection.

Three experimental researches of object detection in the image by the example of face detection task on test set from the base "Yale B" were conducted. In the first experiment, the BODM method was tested with parameters $M_s = 1.1$, $K_r = 1$, $\varphi = 50\%$, $Thr = 2$, the size of minimal sliding window – 24×24 pixels. In the second experiment BODM method was tested with the same parameters as in the first one, applying the previous image processing by BWIF method with parameters $\sigma_d = 1.8$, window size is 11×11, and $\sigma_r = 1.0 \times \hat{\sigma}^2$ at every decomposition level. In the third experiment Viola-Jones method was investigated with parameters $M_s = 1.1$, $K_r = 1$, the size of minimal sliding window – 24×24 pixels. The research results and the example of face detection are shown in fig.7.

Figure 8. Enlarged part of the image from test set of base VNTU-458, processed by BWIF method: a) noisy image; b) denoising image.

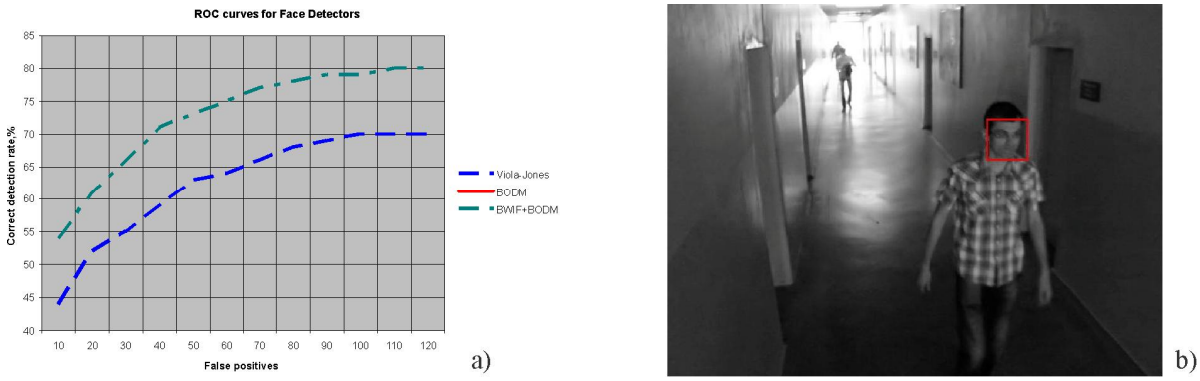

Figure 9. The research results of object detection on test set from the base VNTU-458: a) ROC-curves of detection methods; b) the example of face detection

Three experimental researches of object detection in the image by the example of face detection task on test set from the base "VNTU-458 were conducted. In the first experiment BODM method was tested with the following parameters: $M_s = 1.1$, $K_r = 1$, $\varphi = 50\%$, $Thr = 2$, the size of minimal sliding window – 21×21 pixels. In the second experiment BODM method was tested with the same parameters as in the first one applying the previous image processing by BWIF method with parameters $\sigma_d = 1.8$, window size is 11×11, and $\sigma_r = 1.0 \times \hat{\sigma}^2$ at every decomposition level. In the third experiment Viola-Jones method was tested with the following parameters: $M_s = 1.1$, $K_r = 1$, the size of minimal sliding window – 21×21 pixels. The research results and the example of face detection are shown in fig.8 and fig.9.

5. CONCLUSIONS

The paper presents the object detection method in grayscale images with low light conditions on the example of face detection task. The proposed method consists of two stages: the first is the previous processing of grayscale images by the image denoising method; the second is object detection in grayscale images by the boosting method. Advantages of the proposed method can be summarized as follows:

- increasing object detection rate in proposed boosting method by using modified Haar-like features which combine Haar-like features and symmetrical local binary patterns in comparison with Viola-Jones method;
- increasing object detection rate by combining the proposed boosting method of object detection and the previous processing stage that includes the method of image denoising based on bilateral filter and wavelet thresholding in comparison with proposed boosting method and Viola-Jones method.

Disadvantage of the method is a slight reduction of operation speed because the previous image processing stage is used.

In further researches it is planned to modify the method for processing of color images.

REFERENCES

[1] Lindenbaum, M., Fischer, M. and Bruckstein, A, "On Gabor's contribution to image enhancement," Pattern Recognition 27(1), 1-8 (1994).

[2] Yaroslavsky, L., [Digital picture processing: an introduction], Springer Science & Business Media, Berlin, Heidelberg (1987).

[3] Smith, S.M., and Brady, J.M., "SUSAN – a new approach to low level image processing." International journal of computer vision 23(1), 45-78 (1997).

[4] Tomasi, C., and Manduchi, R., "Bilateral filtering for gray and color images." Proceedings on Sixth International Conference, 839-846 (1998).

[5] Perona, P. and Malik. J., "Scale-space and edge detection using anisotropic diffusion," IEEE Transactions on pattern analysis and machine intelligence 12(7), 629-639 (1990).

[6] Rudin, L., Osher, I.S. and Fatemi, E., "Nonlinear total variation based noise removal algorithms," Physica D: Nonlinear Phenomena 60(1), 259-268 (1992).

[7] Donoho, D.L., and Johnstone, J.M., "Ideal spatial adaptation by wavelet shrinkage," Biometrika 81(3), 425-455 (1994).

[8] Donoho, D.L., "De-noising by Soft-Thresholding," IEEE Transactions on Information Theory 41(3), 613-627 (1995).

[9] Wang, Y. and Zhou H., "Total variation wavelet-based medical image denoising," International Journal of Biomedical Imaging 89095, 1-6 (2006).

[10] Ławicki, T. and Zhirnova, O., "Application of curvelet transform for denoising of CT images," Proc. of SPIE 9662, 966226 (2015).

[11] Buades, A., Coll, B, and Morel, J-M., "A non-local algorithm for image denoising," Proc. IEEE Computer Society Conference on Computer Vision and Pattern Recognition, Vol. 2, 60-65 (2005).

[12] Zhang, M. and Gunturk, B.K., "Multiresolution bilateral filtering for image denoising," IEEE Transactions on Image Processing 17(12), 2324-2333 (2008).

[13] Zhang, Ch. and Zhang, Z., "A survey of recent advances in face detection." Technical Report, Microsoft research, <https://www.microsoft.com/en-us/research/publication/a-survey-of-recent-advances-in-face-detection/> (2010).

[14] Schneiderman, H. and Kanade, T., "Object detection using the statistics of parts," International Journal of Computer Vision 56(3), 151-177 (2004).
[15] Rowley, H.A., Baluja, Sh. and Kanade, T., "Neural network-based face detection," IEEE Transactions on pattern analysis and machine intelligence 20(1), 23-38 (1998).
[16] Viola, P. and Jones, M.J., "Robust real-time face detection." International Journal of Computer Vision 57(2), 137-154 (2004).
[17] Li, S.Z. and Zhang, Z., "Floatboost learning and statistical face detection," IEEE Transactions on pattern analysis and machine intelligence 26(9), 1112-1123 (2004).
[18] Zhang, Ch. Platt, J.C. and Viola P., "Multiple instance boosting for object detection." Advances in Neural Information Processing Systems 18, 1417-1426 (2005).
[19] Forczmański, P. Kukharev, G. Shchegoleva, N. L. "An algorithm of face recognition under difficult lighting conditions," Przegląd Elektrotechniczny 88(10b), 201-204 (2012).
[20] Ojala, T., Pietikainen, M. and Maenpaa, T., "Multiresolution gray-scale and rotation invariant texture classification with local binary patterns," IEEE Transactions on Pattern Analysis and Machine Intelligence 24(7), 971-987 (2002).
[21] Roy, A. and Marcel, S., "Haar local binary pattern feature for fast illumination invariant face detection," Proceedings of the British Machine Vision Conference, 19.1-19-12 (2009).
[22] Gonzalez, R.C. and Woods, R.E., [Digital image processing] Prentice Hall, Upper Saddle River, 350-376 (2002).
[23] Heikkilä, M., Pietikäinen, M. and Schmid C., "Description of interest regions with center-symmetric local binary patterns," Computer vision, graphics and image processing: Lecture Notes in Computer Science 4338, 58-69 (2006).
[24] Masliy, R. and Kulyk, A., "Boosting-Based Face Detection Method" Artificial Intelligence 1, 76-82 (2011).